

Compact surface plasmon amplifier in nonlinear hybrid waveguide*

Shu-shu Wang(王曙曙), Dan-qing Wang(王丹青), Xiao-peng Hu(胡小鹏),
Tao Li(李涛)[†], and Shi-ning Zhu(祝世宁)

National Laboratory of Solid State Microstructures, School of Physics, College of Engineering and Applied Sciences,
Nanjing University, Nanjing 210093, China

(Received 14 April 2016; published online 27 May 2016)

Surface plasmon polariton (SPP), a sub-wavelength surface wave promising for photonic integration, always suffers from the large metallic loss that seriously restricts its practical application. Here, we propose a compact SPP amplifier based on a nonlinear hybrid waveguide (a combination of silver, LiNbO₃, and SiO₂), where a couple of Bragg gratings are introduced in the waveguide to construct a cavity. This special waveguide is demonstrated to support a highly localized SPP-like hybrid mode and a low loss waveguide-like hybrid mode. To provide a large nonlinear gain, a pumping wave input from the LiNbO₃ waveguide is designed to resonate inside the cavity and satisfy the cavity phase matching to fulfill the optical parametric amplification (OPA) of the SPP signal. Proper periods of gratings and the cavity length are chosen to satisfy the impedance matching condition to ensure the high input efficiency of the pump wave from the outside into the cavity. In theoretical calculations, this device demonstrates a high performance in a very compact scheme ($\sim 3.32 \mu\text{m}$) and a much lower pumping power for OPA compared with single-pass pumping. To obtain a comprehensive insight into this cavity OPA, the influences of the pumping power, cavity length, and the initial phase are discussed in detail.

Keywords: surface plasmons, optical parametric amplification, waveguides

PACS: 73.20.Mf, 42.65.Wi, 42.82.Et

DOI: 10.1088/1674-1056/25/7/077301

1. Introduction

Photon, as an information carrier with faster operation speed, lower energy consumption, and higher fault tolerance compared with the electron, has received a great deal of attention in the scientific community. However, the light diffraction limit restricts its applications in integrated devices. Fortunately, surface plasmon polariton (SPP), a bounded optical mode on the interface of metal and dielectric with a smaller wavelength, offers new possibilities for subwavelength photonic integration.^[1] Being accommodated in a metallic part, SPP suffers from the inevitable ohmic loss, which intrinsically restricts its practical applications. Extensive works have been carried out to overcome this barrier. Although using a gain medium to amplify the SPP signal^[2] was considered to be a promising strategy, the widely adopted global pumping determines it to be an inefficient means. Long-range SPP^[3] has been proposed to decrease the loss of the conventional SPP in a passive way, while it needs to sacrifice the field confinement. Besides, the hybrid waveguide^[4–7] combined with dielectric and metal components provided a more optimized solution in balancing the field confinement and the low propagation loss, based on which nanolasers^[4] and compact waveguides^[5] have been realized. It was even proposed to achieve SPP involved second harmonic generation (SHG) in a nonlinear process.^[8] As far as the loss compensation is concerned, the nonlinear process is also a promising means.^[9–12] In our previous

work, an optical parametric amplification (OPA) was proposed with mode matching to compensate and even amplify the SPP signal.^[9] However, due to the relatively low conversion rate, such an OPA only occurs over a long propagation distance and does not benefit enough for a very compact photonic circuitry. Moreover, the totally combined SPP with nonlinear dielectric would bring inconveniences in applicable photonic integration.

To obtain an efficient nonlinear frequency conversion in small dimensions, employing cavity phase matching (CPM) would be a good idea.^[13,14] Here, we propose a new design of plasmonic amplifier in a hybrid waveguide system^[8] with a cavity formed by a couple of Bragg gratings in the waveguides, which takes good advantage of the hybrid modes and the CPM nonlinear process for a compact integration in microns size. Moreover, the whole structure is schemed out by two inputs and two outputs with an in-coupled nonlinear waveguide that splits away after pumping the SPP mode without interfering with the SPP function any more, which would possibly work as a pure amplifier for plasmonic integration.

2. Theoretical model

Figure 1(a) shows the schematic diagram of the nonlinear hybrid plasmonic waveguide. There is a straight SiO₂-loaded silver waveguide coupled with a nonlinear LiNbO₃ (LN) waveguide by two S-bends to form a hybrid waveguide

*Project supported by the National Basic Research Program of China (Grant No. 2012CB921501), the National Natural Science Foundation of China (Grant Nos. 11322439, 11274165, 11321063, and 91321312), the Dengfeng Project B of Nanjing University, China, and the PAPD of Jiangsu Higher Education Institutions, China.

[†]Corresponding author. E-mail: taoli@nju.edu.cn

in the coupling segment. In our theoretical investigation, the dielectric constant of silver is adopted from Ref. [15]. The pumping wave is input from the LN waveguide (with the dimension of $w = h = 500$ nm) with the free space wavelength of $\lambda_p = 890$ nm, and the signal wave is designed as an SPP mode at $\lambda_s = 1780$ nm that propagates in the SiO₂ loaded metal waveguide, where the height and width of the SiO₂ are also 500 nm. The dielectric constant of LN is set as $[\epsilon_x, \epsilon_y, \epsilon_z] = [5.05, 5.05, 4.70]$ and $[4.87, 4.87, 4.54]$ at the wavelengths of 890 nm and 1780 nm, respectively.^[16] In the middle part of the device, the LN waveguide is strongly coupled to the plasmonic one with a very narrow SiO₂ gap (10 nm), which can support hybrid modes, the so-called waveguide-like and SPP-like modes (it is termed as SPP in the following for convenience).^[5] Here, the rectangular LN is defined with its c axis along the z direction. Then a z -polarized input pumping wave (e-light) will be coupled with a y -polarized SPP wave (o-light) in the hybrid part to fulfill a nonlinear process with the second harmonic coefficient (d_{23}) of LN. By numerical simulation with the Lumerical FDTD solution, the propagations of the pumping wave in the LN waveguide and the signal in the SiO₂ loaded plasmonic waveguide are calculated (see Figs. 1(b) and 1(c), respectively), where the pumping wave shows little loss while the SPP appears to have high loss. In the coupling part, two hybrid modes are characterized with mode indices of $n_p = 1.875 + 1.473 \times 10^{-4}i$ and $n_s = 1.777 + 1.631 \times 10^{-3}i$ for the pumping and the signal, whose mode distributions are shown in Figs. 1(d) and 1(e) for the waveguide-like and the SPP-like modes, respectively.

Constructing a cavity by gratings is a matured scheme to amplify the power in distributed Bragg reflector (DBR) lasers.^[17,18] Referring to this method, we introduce a cavity in the hybrid waveguide part by a couple of Bragg gratings, which is designed to play dual roles. One is to enhance the pumping wave intensity inside the cavity under a resonant condition, and the other is, more importantly, to fulfill cavity phase matching (CPM) to achieve an ever constructive nonlinear conversion.^[13] Firstly, we need to find out the optimum structural parameter of the gratings to have strong reflection for the pumping wave and strong transmission for the signal wave. For simplification, the depth of the gratings is chosen to be 250 nm and the duty ratio is 0.5 in every period. Then, a parameter scan is performed by FDTD analysis on a 10-period grating for the reflectance with respect to different periods. Figure 2(a) shows the calculation result; the reflection reaches up to 90% for the pump and is low for the signal ($\sim 20\%$). The data are quite in conformity with our design requirements. Here, for example, the simulated field distributions of the highly-reflected pumping wave and the highly-transmitted signal wave are demonstrated in Figs. 2(b) and 2(c) with the grating of period 600 nm.

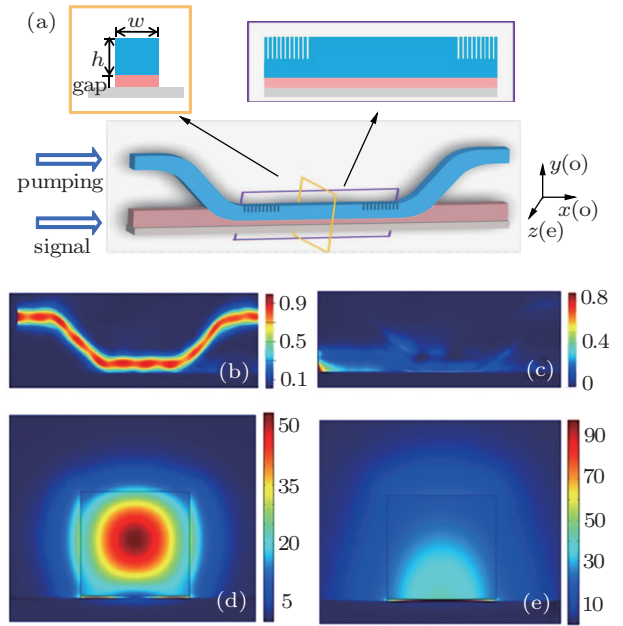


Fig. 1. (color online) (a) Schematic diagram of the nonlinear hybrid plasmonic waveguide. The rectangle nonlinear dielectric is LiNbO₃, the middle part is SiO₂, and the metal is silver. Structural parameters are as follows: $w = h = 500$ nm, gap = 10 nm. For a pumping wave at 890 nm, $[\epsilon_x, \epsilon_y, \epsilon_z](\text{LN}) = [5.05, 5.05, 4.70]$, $n_p = 1.875 + 1.473 \times 10^{-4}i$. For a signal wave at 1780 nm, $[\epsilon_x, \epsilon_y, \epsilon_z](\text{LN}) = [4.87, 4.87, 4.54]$, $n_s = 1.777 + 1.631 \times 10^{-3}i$. The simulated propagating fields of (b) the pump wave from the LN port and (c) the signal wave from the SiO₂ loaded silver port. The lateral field distributions of (d) the pump wave and (e) the signal wave correspond to the waveguide-like and the SPP-like hybrid modes, respectively.

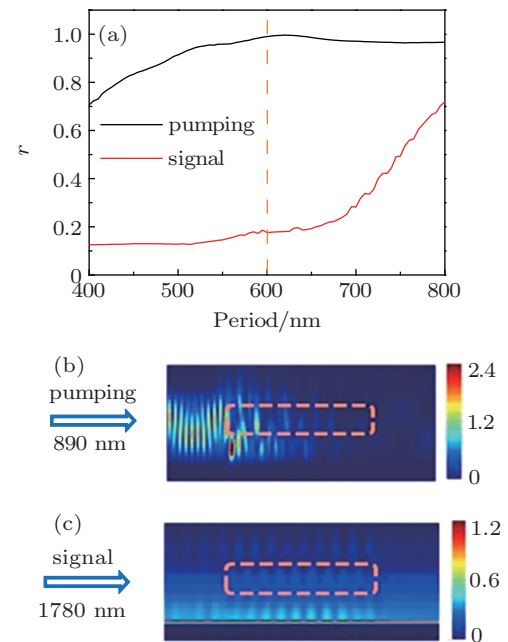


Fig. 2. (color online) (a) The reflectivity of the pump wave (890 nm) and signal wave (1780 nm) as a function of the grating period. The simulated propagating properties of (b) the pump wave and (c) the signal wave with the grating of period 600 nm, where the gratings are indicated by the dashed rectangles.

3. Analysis on nonlinear process

Consider a condition of degenerated signal and idle waves. This pump-resonant OPA process in the cavity can be

well described by the following coupled wave equations:

$$\frac{dA_1}{dx} = -\alpha_1 A_1 + i \frac{\omega_1 \varepsilon_0}{4} \kappa_1 A_1^* A_2 \exp(i(\beta_2 - 2\beta_1)x), \quad (1a)$$

$$\frac{dA_2}{dx} = -\alpha_2 A_2 + i \frac{\omega_1 \varepsilon_0}{4} \kappa_1^* A_1^2 \exp(-i(\beta_2 - 2\beta_1)x), \quad (1b)$$

which describe the interaction of forward-propagating pumping (A_2) and signal waves (A_1),

$$\frac{dB_1}{dx} = -\alpha_1 B_1 + i \frac{\omega_1 \varepsilon_0}{4} \kappa_1 B_1^* A_2 \exp(i(-\beta_2 - 2\beta_1)x), \quad (2a)$$

$$\frac{dB_2}{dx} = \alpha_2 B_2 + i \frac{\omega_1 \varepsilon_0}{4} \kappa_1^* B_1^2 \exp(-i(-\beta_2 - 2\beta_1)x), \quad (2b)$$

which describe the interaction of backward pumping (B_2) and forward signal (B_1). Here, β_1 , β_2 and α_1 , α_2 are the propagation constants and dissipation factors of the signal and pumping waves, respectively. The nonlinear coupling coefficient κ_1 is defined by $\kappa_1 = \iint d_{\text{eff}} \mathbf{E}_p (\mathbf{E}_s^*)^2 dydz$, where \mathbf{E}_p and \mathbf{E}_s are the normalized field distributions of the pump wave and the signal wave. Defining $\Delta\beta$ ($\Delta\beta = \beta_2 - 2\beta_1$) as the wave-vector mismatch, we can obtain the coherence length L_c as $\pi/\Delta\beta$, which equals 4.5266 μm according to our calculation. To guarantee an efficient OPA process, we exploit the cavity-phase-matching condition^[13] that the cavity length should be less than L_c or around an odd number of times of L_c . Meanwhile, the cavity is set to be resonant for the pump wave, which requires that the cavity length (L) should satisfy $2\beta_2 L = 2m\pi$ (m is a positive integer), then the pump wave can be coherently enhanced. By defining $l_0 = \pi/\beta_2$ as the characteristic length, then $L = ml_0$. The phase shift from the reflection of the Bragg gratings is π .

According to the above analyses, we are ready to calculate the OPA process within the hybrid waveguide when the proper cavity parameters are determined with specific cavity length, reflectance of gratings, and initial condition of input pumping and signal waves. In fact, to obtain a high coupling efficiency from the input pumping to the cavity, the parameters of the cavity structure need to be carefully chosen to meet the impedance matching condition,^[19] which will be particularly discussed later. Here, we would like to show the result first with properly designed parameters. The cavity length is chosen to be 14 times of the characteristic length l_0 (i.e., $\sim 3.32 \mu\text{m}$), which is less than L_c , satisfying the CPM condition. Proper periods of 495 nm ($\sim 95\%$ for pump) and 600 nm ($\sim 99\%$ for pump) are chosen for the front and rear gratings respectively to ensure the impedance matching^[19] for an efficient input coupling. The initial phase difference between the pump and the signal is set to be π , which is an optimal initial condition (see later for a detailed discussion). At the beginning, an input pumping power of 10 W is set to investigate the nonlinear conversion process for a signal seed with the power of 0.001 W, where the contributions of the forward and backward pumping can be conveniently calculated by Eqs. (1) and (2). It is shown in Fig. 3(a) that the forward pumping amplifies the signal wave greatly in a CPM process while the backward pump wave contributes little in despite of a slight

decay and tiny oscillations. It is ready to accept that the coherent nonlinear process only occurs as long as the phase matching condition is satisfied. By combining these two processes together, the OPA for the SPP wave inside the cavity of the hybrid waveguide ($L = 14l_0 \approx 3.32 \mu\text{m}$) can be numerically calculated, as shown in Fig. 3(b) (the black curve). In order to demonstrate the advantage of the CPM OPA effect, a single-pass pumping without cavity and a solely lossy SPP without pumping are also calculated for comparison, which are displayed as red and blue curves in Fig. 3(b), respectively. It is observed that the SPP signal decays by 3.75% after propagating $\sim 3.32 \mu\text{m}$ without any pumping due to the mode loss. A single-pass pumping process will compensate some loss with 1.53% attenuation. This low nonlinear efficiency is due to the low pumping power which has not reached the OPA threshold. Impressively, with the same input pumping power, the signal increases by 5% with the cavity introduced, which clearly shows the high efficiency of the CPM OPA in the cavity of the hybrid waveguide. Here, the change of the effective refractive index induced by the pump power through photorefractive is negligible.

As far as the threshold is concerned, the amplification factor of the signal wave with respect to the input pumping power is investigated for the cases with and without the cavity, the results are shown in Fig. 3(c). It is found that a 28 W pumping power is needed to achieve the amplification ($P_s/P_s(0) > 1$) without cavity, while it is much lower (1.28 W) when a cavity is introduced. In fact, although the energy of the pumping wave does transfer to the signal wave even when the incident power is lower than the threshold, this nonlinear gain is too small to compensate for the loss of the signal wave.

It is worth noting that the pump wave is input from outside of the cavity where the front grating has a high reflectance. To obtain a high input efficiency, the reflection of the two gratings of the cavity should be carefully designed to meet impedance matching.^[19] Here, we define r_1 and r_2 as the power reflectivity of the front and the rear gratings, t is the transmission of the pump wave propagating inside the cavity including the propagating loss, and t_{NL} is the additional nonlinear transmission term including the consumption of nonlinear conversion process. Then the cavity reflectance parameter can be expressed as $r_m = t^2 t_{\text{NL}} r_2$. As indicated, r_m depends on the incident pump power through t_{NL} and the cavity length through t . If $r_1 = r_m$, the incident power can be efficiently coupled into the cavity. This is the impedance matching condition. All the previous data are calculated under this condition. To show its influence, the OPA effect is compared by varying r_2 with different r_1 , as displayed in Fig. 3(d). Here the black curve corresponds to the impedance matching condition, which gives the best amplification. The red and blue lines correspond to $r_1 = 0.96$ and 0.99, respectively. It is seen that the $r_1 = 0.96$ condition (red curve) is quite close to the impedance matching condition. While the higher reflectance ($r_1 = 0.99$) manifests lower OPA efficiency, because it is farther away from impedance matching.

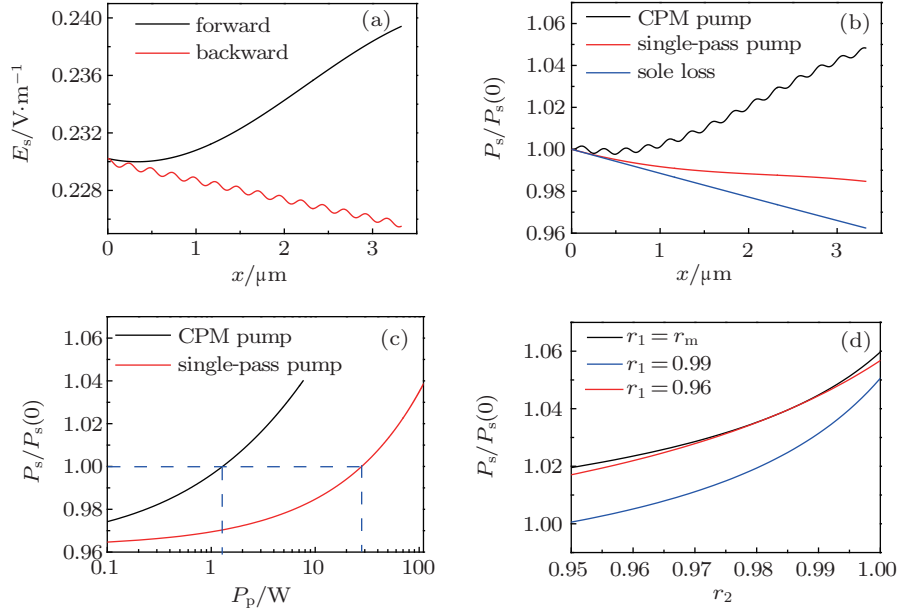


Fig. 3. (color online) (a) Evolution of the signal wave field being pumped by forward and backward components of the pumping wave within a cavity of $L = 14l_0 \approx 3.32 \mu\text{m}$. (b) Power evolution of the signal wave within a propagation distance of $3.32 \mu\text{m}$ for CPM pumping, single-pass pumping, and without pumping. (c) The output power of the signal wave varies with the input pumping power with cavity and without cavity, where the thresholds P_p are marked out for the OPA gain condition ($P_s/P_s(0) = 1$). (d) The output power of the signal wave varies with r_2 for the cases of $r_1 = r_m$, 0.99, and 0.96.

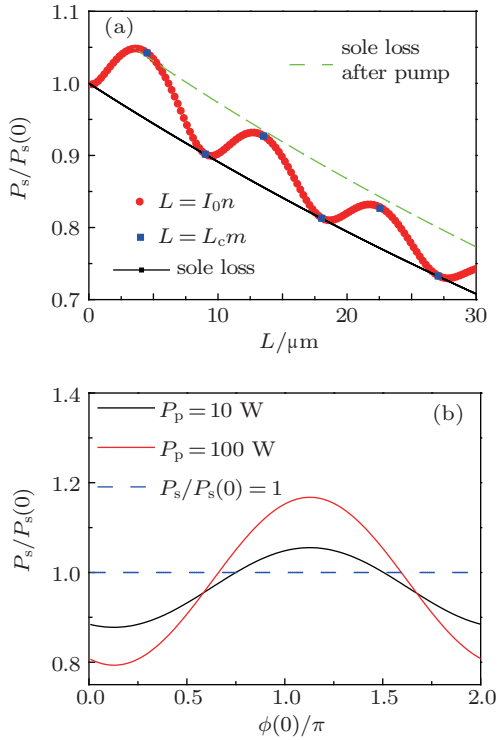


Fig. 4. (color online) (a) The OPA performance with respect to different cavity lengths at the pumping power of 10 W, where the propagation of solely lossy SPP (black curve), the signal in cavity with lengths of resonant length (red circle) and integer number times L_c (blue square), and lossy SPP after being pumped by a $3.32 \mu\text{m}$ cavity (green curve) are presented. (b) The output power of the signal wave varying with the initial phase difference at different pumping powers.

Since the influence of the pumping power on the OPA process is investigated, it is reasonable to check another factor: the cavity length on the OPA performance. We adopt Eqs. (1) and (2) to calculate the evolution of the output signal power as a function of the cavity length with the input

signal of 0.001 W and pump of 10 W. Here, r_2 is set at 0.99 and r_1 is chosen according to impedance matching ($r_1 = r_m$). Figure 4(a) displays the OPA results, showing that the maximum signal outputs are not obtained rightly at the coherent length and odd times of it but with a little shift. Because r_2 is fixed while r_1 (i.e., r_m) is resolved by the length of the cavity, then the enhancement of the pumping power inside the cavity is influenced by the cavity length. However, the minima of the signal output locate exactly at the cavity lengths of even times of the coherent length. It is because no matter how much pumping power is in the cavity, the nonlinear conversion power from the pump wave to the signal wave is zero with the cavity lengths of even times of the coherent length, which actually is equivalent to the solely lossy SPP propagation (the black one). The green dashed curve shows the SPP propagation pumped by a $3.32 \mu\text{m}$ cavity, which is higher than not only the black curve (the solely lossy SPP) but also the red dot one (the cases of longer cavities). It means that the $3.32 \mu\text{m}$ cavity is an optimized amplifier in this occasion which weakens the attenuation of the SPP wave to some extent.

In the above investigations, the initial phase difference between pumping and signal is assumed to be π to ensure a high proportion of the pump energy flowing to the signal. In fact, the initial phase difference is important in the energy transfer direction in the nonlinear process. We study the relation between the output power of the signal wave and the initial phase difference in the CPM OPA process. We calculate the output power of the signal wave as a function of the initial phase difference $\phi(0)$ at pumping of 10 W and 100 W and the input signal of 0.001 W within an optimum cavity

($L = 14l_0 \approx 3.32 \mu\text{m}$), the results are shown in Fig. 4(b). As has been mentioned before, there is an optimum phase condition of $\phi(0)$ around π to achieve the maximum OPA. Besides, it is found that the OPA condition ($P_s/P_s(0) > 1$) allows a considerable range of $\phi(0)$, which becomes broader with increasing pumping power. In total, these results reveal the fact that this compact SPP amplifier has a considerable tolerance to the initial phase difference between the signal and pumping, though it indeed plays an important role.

4. Conclusion

A compact SPP amplifier is proposed based on a nonlinear hybrid waveguide with a two-input and two-output coupler configuration, where cavity phase matching is introduced to enhance the OPA process without domain engineering. By employing the impedance matching to efficiently couple the pumping wave from outside into the cavity, it is found that in this very compact scheme ($\sim 3.32 \mu\text{m}$ for the optimum cavity), the threshold of the pumping power for CPM OPA is reduced by one order of magnitude compared to that of single-pass OPA. In addition, the OPA performance with respect to different pump power, grating reflection, cavity length, and initial phase are analyzed and discussed. This compact scheme for SPP amplification would provide a new approach in the future photonic integration.

References

- [1] Barnes W L, Dereux A and Ebbesen T W 2003 *Nature* **424** 824
- [2] Leon I D and Berini P 2008 *Phys. Rev. B* **78** 161401(R)
- [3] Burke J J, Stegeman G I and Tamir T 1986 *Phys. Rev. B* **33** 5186
- [4] Oulton R F, Sorger V J, Zentgraf T, Ma R M, Gladden C, Dai L, Bartal G and Zhang X 2009 *Nature* **461** 629
- [5] Oulton R F, Sorger V J, Genov D A, Pile D F P and Zhang X 2008 *Nat. Photon.* **2** 496
- [6] Holmgaard T and Bozhevolnyi S 2007 *Phys. Rev. B* **75** 245405
- [7] Holmgaard T, Gosciniaik J and Bozhevolnyi S 2010 *Opt. Express* **18** 23009
- [8] Lu F F, Li T, Hu X P, Cheng Q Q, Zhu S N and Zhu Y Y 2011 *Opt. Lett.* **36** 3371
- [9] Lu F F, Li T, Xu J, Xie Z D, Li L, Zhu S N and Zhu Y Y 2011 *Opt. Express* **19** 2858
- [10] Simon H J, Mitchell D E and Watson J G 1974 *Phys. Rev. Lett.* **33** 1531
- [11] Simon H J, Benner R E and Rako J G 1977 *Opt. Commun.* **23** 245
- [12] Palomba S and Novotny L 2008 *Phys. Rev. Lett.* **101** 056802
- [13] Xie Z D, Lv X J, Liu Y H, Ling W, Wang Z L, Fan Y X and Zhu S N 2011 *Phys. Rev. Lett.* **106** 083901
- [14] Armstrong J A, Bloembergen N, Ducuing J and Pershan P S 1962 *Phys. Rev.* **127** 1918
- [15] Johnson P B and Christy R W 1972 *Phys. Rev. B* **6** 4370
- [16] Edwards G J and Lawrence M 1984 *Opt. Quantum Electron.* **16** 373
- [17] Akulova Y A, Fish G A, Koh P C, Schow C L, Kozodoy P, Dahl A P, Nakagawa S, Larson M C, Mack M P, Strand T A, Coldren C W, Hegblom E, Penniman S K, Wipiejewski T and Coldren L A 2002 *IEEE J. Sel. Top. Quantum Electron.* **8** 1349
- [18] Jayaraman V, Chuang Z M and Coldren L A 1993 *IEEE J. Quantum Electron.* **29** 1824
- [19] Kozlovsky W J, Nabors C D and Byer R L 1988 *IEEE J. Quantum Electron.* **24** 913